# Electrochemical Reduction of Nitrite and Nitric Oxide Catalyzed by an Iron–Alizarin Complexone Adsorbed on a Graphite Electrode

**Jiujun Zhang, A. B. P. Lever,* and William J. Pietro**

Department of Chemistry, York University, North York (Toronto), Ontario, Canada M3J 1P3

*Received September 22, 1993**

The ligand alizarin complexone, [((3,4-dihydroxy-2-anthraquinolyl)methyl)imino]diacetic acid is strongly and irreversibly adsorbed on graphite electrode surfaces and binds ferric ions to form surface-bound metal complexes. Upon reduction, the adsorbed complex is an active electrocatalyst for the reduction of both nitrite and nitric oxide. A rotating platinum ring–graphite disk electrode was employed to detect *in situ* the products of nitrite reduction. The main products of this electrocatalytic nitrite reduction are believed to be $NH_2OH$ and $NH_3$. Adducts formed between substrate and adsorbed catalyst are formed in the initial steps of the reduction on the basis of surface cyclic voltammetric behavior. The possible application of this electrocatalytic reduction in the analysis of nitrite and nitric oxide is also discussed. Four other ligands, xylenol orange, methylthymol blue, fluorexon, and thymolphthalein complexone, which have the same coordination structure of a (methylimino)diacetate group and an adjacent aromatic hydroxyl group, were also electrocatalysts for nitrite reduction.

## Introduction

The electrochemical and conventional catalytic reduction of nitrite and nitric oxide are problems of special interest from basic,[1] biological,[2] energetic,[3] and environmental[1] viewpoints. Much effort has been made to explore metal–ligand complex catalysts which can be coated on electrode surfaces to catalyze the reduction of $[NO_2]^-$ and NO, such as iron, ruthenium EDTAs and porphyrins,[4–12] nickel, cobalt cyclam,[13–15] iron polyoxotungstates,[16] and osmium bipyridyls.[17] On the basis of the electrochemical, spectroscopic, and product determination data, several different reduction models for the aforementioned redox processes have been proposed reflecting a range of complex mechanisms. We recently discovered that alizarin complexone (**1**) (abbreviated as AC), an alizarin derivative, forms an iron complex, $Fe^{III}(AC)$ (**2**) (Figure 1) which is an effective electrocatalyst for $[NO_2]^-$ or NO reduction when the catalyst is adsorbed on graphite electrodes.

The surface electrochemistry of **2** and its catalytic activities for $O_2$ and $H_2O_2$ reduction were examined most recently by Anson and co-workers,[18] and the importance of the surface coordination

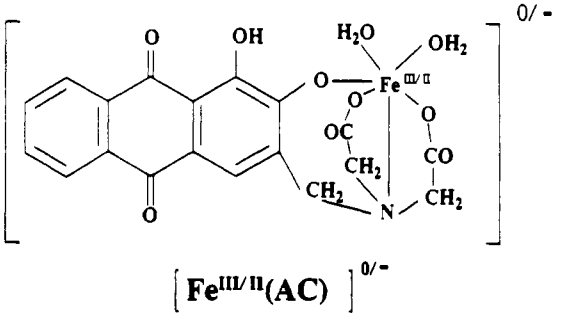


**Figure 1.** Proposed structure of the iron alizarin complexone.[21]

structure of $Fe^{III}$ with a (methylimino)diacetate group and an adjacent aromatic hydroxyl group for the catalytic activity of substrate reduction was emphasized.

We describe here such a strongly adsorbing, electroactive chelating alizarin ligand derivative which binds $Fe^{III}$ ions at the electrode surface to produce an effective electrocatalyst for $[NO_2]^-$ and NO reduction. A ring–disk electrode was used to detect, *in situ*, the main product of $[NO_2]^-$ reduction. In order to demonstrate the importance of the surface coordination structure of $Fe^{III}$ with this ligand, four other strongly adsorbing, chelating, ligands which bind in a similar fashion to $Fe^{III}$ were also tested as electrocatalysts for nitrite reduction.

## Experimental Section

**1. Materials.** Alizarin complexone (Aldrich) was recrystallized twice from ethanol. Sodium nitrite and nitric oxide were reagent grade from Aldrich and were used without further purification. Other reagent grade chemicals were used as received.

All solutions were prepared from doubly distilled water which was further purified by passage through a purification train. Nitrite solutions prepared from $NaNO_2$ were calibrated by titration with standard 0.05 M $KMnO_4$ + 0.1 M $H_2SO_4$ solution. The pH of the solutions was controlled with $CH_3COOH/CH_3COONa$ buffers which were added to the 0.1 M $NaClO_4$ supporting electrolyte. Solutions were deaerated by bubbling with pure argon gas (99.99%).

Complexes of the ligand with $Fe^{III}$ or $Fe^{II}$ ions were prepared by mixing $Fe(NO_3)_3$ or $FeCl_2$ with alizarin complexone in the molar ratio of 1:1 in 0.1 M $NaClO_4$ + 0.1 M $CH_3COOH/CH_3COONa$ buffer aqueous solution (pH 5.3). The continuous-variation method was employed to determine the coordination number between $Fe^{III}$ or $Fe^{II}$ ion and alizarin complexone.

* Abstract published in *Advance ACS Abstracts,* February 15, 1994.

(1) Basolo, F.; Burwell, R. L., Jr. *Catalysis: Progress in Research*; Platinum Press: New York, 1973.
(2) Losada, M. *J. Mol. Catal.* **1975**, *1*, 245.
(3) Langer, K. H.; Pate, K. *Nature* **1980**, *284*, 434.
(4) Ochiyama, S.; Muto, G. *J. Electroanal. Chem. Interfacial Electrochem.* **1981**, *127*, 275.
(5) Ogura, K.; Ishikawa, H. *J. Chem. Soc., Faraday Trans. 1* **1980**, *80*, 2243.
(6) Ogura, K.; Ishikawa, H. *Electrochim. Acta* **1983**, *28*, 167.
(7) Rhodes, M. R.; Barley, M. H.; Meyer, T. J. *Inorg. Chem.* **1991**, *30*, 629.
(8) Barley, M. H.; Takeuchi, K.; Murphy, W. R., Jr.; Meyer, T. J. *J. Chem. Soc., Chem. Commun.* **1985**, 507.
(9) (a) Barley, M. H.; Takeuchi, K. J.; Meyer, T. J. *J. Am. Chem. Soc.* **1986**, *108*, 5876. (b) Barley, M. H.; Rhodes, M. R.; Meyer, T. J. *Inorg. Chem.* **1987**, *26*, 1746.
(10) Rhodes, M. R.; Meyer, T. J. *Inorg. Chem.* **1988**, *27*, 4772.
(11) Chen, S. M.; Su, Y. O. *J. Electroanal. Chem. Interfacial Electrochem.* **1990**, *280*, 189.
(12) Hayon, J.; Raveh, A.; Bettelheim, A. *J. Electroanal. Chem. Interfacial Electrochem.* **1993**, *359*, 209.
(13) Younathan, J. N.; Wood, K. S.; Meyer, T. J. *Inorg. Chem.* **1992**, *31*, 3280.
(14) Taniguchi, I.; Nakashima, N.; Matsushita, K.; Yasukouchi, K. *J. Electroanal. Chem. Interfacial Electrochem.* **1987**, *224*, 199.
(15) Li, H. L.; Chamber, J. Q.; Hobbs, D. T. *J. Electroanal. Chem. Interfacial Electrochem.* **1988**, *256*, 447.
(16) Toth, J. E.; Anson, F. C. *J. Am. Chem. Soc.* **1989**, *111*, 2444.
(17) Doherty, A. P.; Vos, J. G. *J. Chem. Soc., Faraday Trans.* **1992**, *88*, 2903.
(18) Zhang, J. J.; Anson, F. C. *J. Electroanal. Chem. Interfacial Electrochem.* **1993**, *353*, 265.

0020-1669/94/1333-1392$04.50/0 

Job's plots were obtained by keeping the total concentration of $Fe^{III}$ ion and ligand constant, ca. $C_{Fe^{III}} + C_{AC} = 0.015$ M, and the total concentration of $Fe^{II}$ ion and ligand constant, ca. $C_{Fe^{II}} + C_{AC} = 0.03$ M in 0.1 M $NaClO_4$ + 0.1 M $CH_3COONa/CH_3COOH$ buffer solutions (pH 5.3). The absorbance was measured at 554 nm in both cases.

**2. Procedures and Apparatus.** Basal plane pyrolytic graphite (BPG) electrodes (Union Carbide) were sealed to stainless steel shafts with heat-shrinkable polyolefin tubing. The electrodes, mounted with the basal planes of the graphite exposed, were polished using a 0.5-$\mu$m alumina suspension, sonicated for 5 min in water and rinsed with acetone and water before each experiment. The area of electrode, 0.17 $cm^2$, was calibrated by using solutions of $1 \times 10^{-3}$ M $[Fe(CN)_6]^{3-}$.

The surface-bound $Fe^{III}(AC)$ (**2**) modified electrode could be prepared from ligand **1** by three different methods. (i) A freshly polished electrode was soaked in a dilute solution of $Fe^{III}(AC)$ (ca. $1 \times 10^{-4}$ M) for about 10 s and then washed and transferred to pure supporting electrolyte to record the cyclic voltammograms; (ii) a clean polished electrode was first soaked in a solution of ligand **1** ($1 \times 10^{-4}$ M) for several seconds and then washed and exposed to a solution of $1 \times 10^{-4}$ M $Fe(NO_3)_3$ + 0.1 M $NaClO_4$ buffered at pH 5.3 for 20 s; or (iii) the ligand-preadsorbed electrode was transferred to a electrolyte solution containing dilute ($5 \times 10^{-5}$ M)$Fe(NO_3)_3$ buffered at pH 5.3. When the cyclic voltammograms were recorded, with multiple cycles between the potential range of 0.0 to –0.4 V, the $Fe^{III}/Fe^{II}$ wave would gradually grow with time, indicating formation of the surface complex.

The electrodes coated by complexes of the $Fe^{III}$ ion with the other four ligands, xylenol orange, methylthymol blue, fluorexon, and thymolphthalein complexone, were also prepared by the methods described above.

Electrochemical measurements were performed with conventional three-compartment cells. For cyclic voltammetry and rotating ring–disk voltammetry an RDE 3 potentiostat (Pine Instruments) and ASR rotator (Pine Instruments) were employed with an X-Y recorder. The ring–disk electrode consisted of a pyrolytic graphite disk and a platinum ring. A collection efficiency of 0.15 was calibrated by experiments with solutions of $[Fe(CN)_6]^{3-}$. For estimation of the number of electrons involved in the reduction processes, the diffusion coefficient[19] for $[NO_2]^-$, $1.5 \times 10^{-5}$ $cm^2$ $s^{-1}$, was used.

For the purpose of *in situ* detection of products produced during the electrocatalytic reduction of $[NO_2]^-$, the oxidation of $NH_2OH$, $NH_2$-$NH_2$, and $[NO_2]^-$ on a platinum ring of a rotating ring (Pt)–disk (graphite) electrode was recorded. In the study of the oxidation of these substrates at the ring electrode, the graphite disk electrode was open circuit. In this way, current–potential curves were obtained for the corresponding substrate, allowing determination of the potential range to be used to polarize the ring electrode for *in situ* detection of nitrite reduction products.

During the detection of the possible products of electrocatalytic reduction of nitrite, the graphite disk electrode, coated with catalyst, was scanned in the potential range 0.2 to –1.0 V and the platinum ring electrode was fixed at a potential where $NH_2NH_2$ or $NH_2OH$ could be oxidized.

All experiments were carried out at ambient laboratory temperature. The potentials were measured and are quoted with respect to a saturated calomel electrode.

## Results and Discussion

**1. Surface Electrochemistry of the Adsorbed $Fe^{III}(AC)$ Complex.** The proposed structure for the solution species based upon previous characterization[18,21] is shown in Figure 1, and we suppose, given the similarity between the surface and solution voltammetry (below) that the surface species is still a 1:1 complex, similar to that in solution. Figure 2 shows cyclic voltammetric data for the adsorbed $Fe^{III}(AC)$ complex on an BPG electrode. In pure electrolyte (no $Fe^{III}(AC)$ in solution) two waves are observed attributed to surface responses, with current linearly proportional to scan rate (Figure 3). On the basis of the charge under couples I and II, the coverage is approximately one monolayer, $3 \times 10^{-10}$ mol $cm^{-2}$, assuming the entire surface is electroactive.

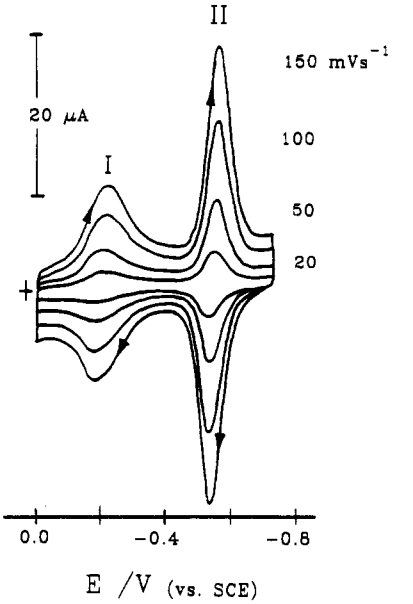


**Figure 2.** Cyclic voltammograms of $Fe^{III}(AC)$ adsorbed on a graphite electrode. The freshly polished electrode was soaked in $1 \times 10^{-4}$ M $Fe(NO_2)_3$ + $1 \times 10^{-4}$ M AC (buffered by 0.1 M acetate/acetic acid solution, pH 5.3) for 10 s, washed, and transferred to pure supporting electrolyte (0.1 M $NaClO_4$ + 0.1 M $CH_3COOH/CH_3COONa$ buffer solution at pH 5.3) to record the voltammograms. Potential scan rates were as marked in the figure.

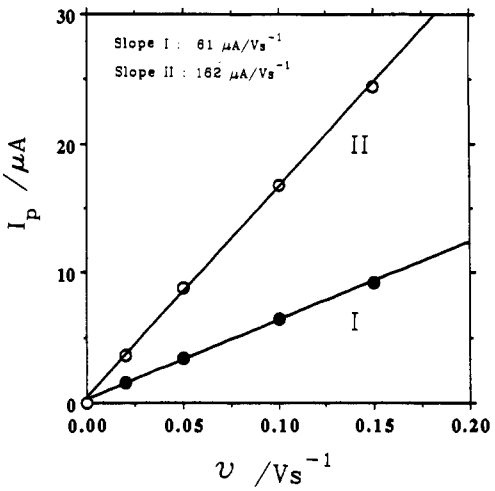


**Figure 3.** Potential scan rate dependence of the current of couples I and II in Figure 1.

The more positive wave, I, with a half-bandwidth of ca. 125 mV and a peak to peak separation of ca. 50 mV, is the 1-electron $Fe^{III}/Fe^{II}$ process in the adsorbed complex, and the less positive wave, II, with a half-bandwidth of ca. 60 mV and a peak to peak separation of 30 mV is a 2-electron reduction of the quinonoid ligand **1**.[18] The potential positions of these two waves (I, –0.20 V; II, –0.55 V) are approximately identical to those observed in the solution voltammetry of the $Fe^{III}(AC)$ species (I, –0.20 V; II, –0.56 V).[18] The broader half-bandwidths of these two waves (I, 125 mV; II, 60 mV) compared to those expected theoretically for a reversible reactant confined to the electrode surface (90.6 mV for a 1-electron process and 45.3 mV for a 2-electron process) and the relatively large peak to peak separation reflect that the electrochemical behavior of the adsorbed $Fe^{III}(AC)$ is not fully Nernstian.[20] The ratio of the two slopes of the lines for waves I and II, shown in Figure 3, slope II/slope I, is 2.6 instead of 4 which would be expected from Nernstian behavior of a surface reactant.

The area under voltammetric peak I is about 45–50% as large as that under the peak for the 2-electron process, II, demonstrating

(19) Zaytsev, I. O.; Aseyev, G. G. *Properties of Aqueous Solutions of Electrolytes*; CRC Press: Boca Raton, FL, 1992; p 975.
(20) Bard, A. J.; Faulkner, L. R. *Electrochemical Methods. Fundamentals and Applications*; John Wiley & Sons: New York, 1980.
(21) (a) Leonard, M. A.; West, T. S. *J. Chem. Soc.* **1960**, 4477. (b) Qureshi, G. A.; Ireland, N. *Bull. Chim. Soc. Belg.* **1981**, *90*, 9.

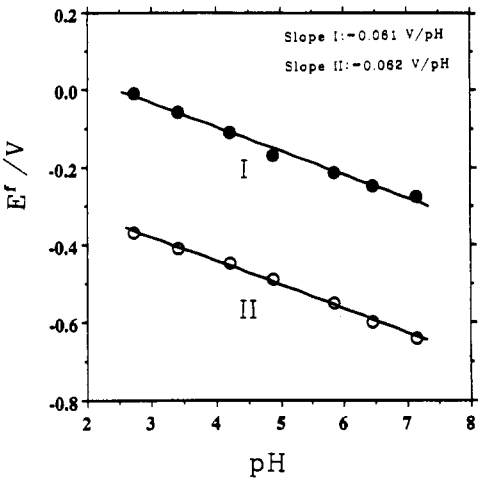


**Figure 4.** Formal potentials of waves I and II from Figure 1 as a function of pH. Supporting electrolyte: 0.1 M $NaClO_4$ + 0.1 M $CH_3COOH$/$CH_3COONa$ buffer. The solution pH was changed by adding aliquots of 1 M NaOH or 1 M $HClO_4$. Potential scan rate: 100 mV $s^{-1}$.

that each adsorbed ligand molecule coordinates one $Fe^{III}$ ion to form a complex having the same composition as the complex obtained when two reactants are mixed in solution, as shown by a Job's plot measured in a solution buffered at pH 5.3.[18]

The pH dependences of the formal potentials of both waves in Figure 1 are shown in Figure 4; both lines have a slope of approximately -60 mV/pH, signifying that the half-electrochemical reactions have unit ratio of electron and proton involved. Note that the complex decomposes in an environment of pH less than 2 or more than 8.

For wave I ($Fe^{III}/Fe^{II}$ center), the most likely half-reaction which accommodates the pH dependence shown in Figure 4 is

$$[Fe^{III}(AC)(H_2O)(OH)]^- + e^- + H^+ \leftrightarrow [Fe^{II}(AC)(H_2O)_2]^- \quad (1)$$

In the $Fe^{III}$(AC) complex **2**, the ligand, **1**, is almost certainly tetradentate, leaving two coordination sites on the $Fe^{III}$ center to be occupied by $H_2O$ molecules (Figure 1),[18,21] consistent with (1).

Wave II (Figure 2) which, from the charge analysis, involves 2 electrons, is ascribed to

$$[Fe^{II}(AC)(H_2O)_2]^- + 2e^- + 2H^+ \leftrightarrow [Fe^{II}(ACH_2)(H_2O)_2]^- \quad (2)$$

also being consistent with the pH dependence.

**2. Catalysis of the Reduction of $[NO_2]^-$ by the Adsorbed $Fe^{III}$(AC) Complex.** The irreversibly adsorbed $Fe^{III}$(AC) complex displays an effective electrocatalytic activity for the reduction of $[NO_2]^-$ anion. Neither the bare electrode nor the free ligand-modified electrode shows any catalytic activity for $[NO_2]^-$ reduction, as shown in Figure 5A,B. However, the $Fe^{III}$(AC)-coated electrode exhibits very strong catalytic activity for the reduction of $[NO_2]^-$, as shown in Figure 5C,D. The sharpness of the catalytic current beginning around -0.6 to -0.7 V reflects a high reduction rate. Note that the wave near -0.55 V is the response, II, from the adsorbed complexed ligand.

The catalytic reduction curves (Figure 5C,D) are clearly composed of two waves, similar to those reported by Uchiyama and Muto[4] for the reduction of $Fe^{II}$–EDTA–NO complexes. When the potential is switched beyond -0.7 V and scanned back, a crossover appears in the cyclic voltammogram, characteristic of the formation, at the electrode surface, of a product which is itself reducible at a potential just negative of the nitrite reduction process. Note that if a rotating disk electrode is used, this product is "spun away" and a crossover does not appear (vide infra).

When the system is scanned repeatedly, negative of the nitrite reduction process, the catalytic current diminishes on each

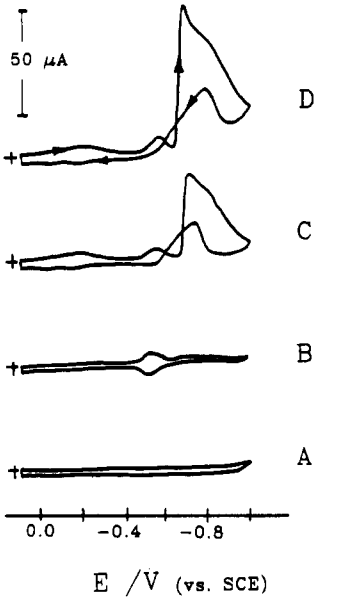


**Figure 5.** Cyclic voltammograms for the reduction of $[NO_2]^-$ at a graphite electrode: (A) bare electrode in 5 × $10^{-4}$ M $NaNO_2$; (B) electrode with adsorbed ligand **1** in 5 × $10^{-4}$ M $NaNO_2$; (C) $Fe^{III}$(AC) (**2**) modified electrode by 3 × $10^{-10}$ mol $cm^{-2}$ $Fe^{III}$(AC) in 5 × $10^{-4}$ M $NaNO_2$; (D) $Fe^{III}$(AC) (**2**) modified electrode by 3 × $10^{-10}$ mol $cm^{-2}$ $Fe^{III}$(AC) in 1 × $10^{-3}$ M $NaNO_2$. Supporting electrolyte was as in Figure 1 (pH 5.3) (first scan). Potential scan rate: 20 mV $s^{-1}$.

successive cycle. Wave I ($Fe^{III}/Fe^{II}$ couple) also diminishes, but wave II (ligand redox) is unaffected. Thus, iron is lost from the active surface on successive scans, but the ligand remains adsorbed. If an iron-depleted electrode is exposed to additional $Fe^{III}$ ions and polarized at about +0.2 V for 1 min, the electrocatalytic activity is fully restored, at least for the first reduction cycle. Unfortunately the electrode surface is not replenished with iron when exposed to $Fe^{III}$ ions and polarized negative of the nitrite reduction process; thus this does not provide a mechanism to inhibit iron loss. Preliminary studies to coat the electrode to inhibit iron loss have not yet been successful in inhibiting iron loss yet retaining electrocatalytic activity.

Another significant feature is that the potential of catalytic reduction of $[NO_2]^-$ (around -0.6 to -0.7 V) is more negative than the formal potential of catalyst ($Fe^{III}/Fe^{II}$ center, -0.2 V) and more negative than the reduction of the ligand (couple II, -0.55 V). On the basis of previous extensive literature analysis of systems of this kind,[4-17] it is probable that the reduction of nitrite ion occurs at a potential corresponding with the reduction potential of an adduct formed between the reduced substrate and catalyst (see below).

Cyclic voltammograms were recorded at different scan rates as shown in Figure 6. Good linearity was observed between the first peak height (current) and the square root of scan rate (Figure 7A) (each scan a new surface). The relationship between peak potential and logarithm of scan rate (Figure 7B) can be used to estimate roughly the number of electrons involved in the catalytic reduction.[20] Because of loss of iron from the surface, it is not practical to analyze the number of electrons involved in the reduction at more negative potentials. For a totally irreversible electrochemical reduction, the peak current in the cyclic voltammograms can be expressed as[20]

$$i_p = (2.99 \times 10^5) n(\alpha n_\alpha)^{1/2} A C_0 D_0^{1/2} v^{1/2} \quad (3)$$

where $i_p$ is the peak current (amperes), $n$ is the number of electrons involved in the reduction. $\alpha n_\alpha$ is a parameter reflecting the irreversibility of the reduction, $A$ is the area of the electrode ($cm^2$), $C_0$ is the concentration of substrate (mol $cm^{-3}$), and $v$ is the potential scan rate (V $s^{-1}$), $D_0$ is the diffusion coefficient of substrate ($cm^2$ $s^{-1}$). When $A$, $C_0$, and $D_0$ are known, the value of $n(\alpha n_a)$ can be calculated from the slope of the line shown in

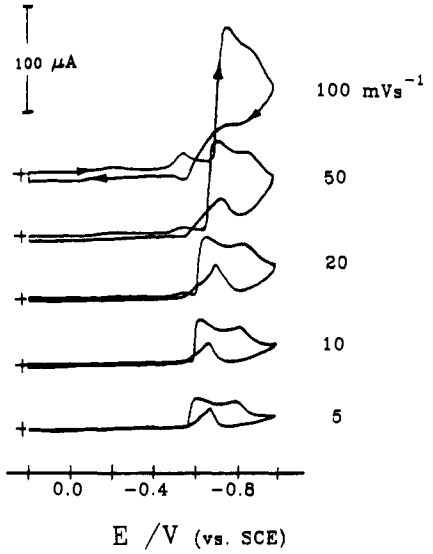


**Figure 6.** Cyclic voltammograms for the reduction of $8 \times 10^{-4}$ M $NaNO_2$ at a species **2** modified graphite electrode containing $3 \times 10^{-10}$ mol cm$^{-2}$ $Fe^{III}(AC)$. Supporting electrolyte was as in Figure 1 (pH 5.3) (first scan). Potential scan rates were as marked in the figure.

Figure 7A. On the other hand, the peak potential in cyclic voltammograms can be expressed as a function of the logarithm of the scan rate:[20]

$$E_p = E^f - (RT/\alpha n_\alpha F)[0.78 + \ln(D_0/k_0)^{1/2} + \ln(\alpha n_\alpha F v^{1/2}/RT)] \quad (4)$$

at 25 °C

$$E_p = k - (0.03/\alpha n_\alpha)\log(v) \quad (5)$$

where $k$ is a constant related to $R$, $T$, $F$, $D_0$, $E^f$ (formal potential), and $k_0$ (standard heterogeneous rate constant). On the basis of eq 3, the value of $\alpha n_a$ can be estimated from the slope of the line shown in Figure 7B. Therefore the number of electrons, $n$, involved in the reduction process can be obtained from data shown in Figure 7A,B; a value of $n = 4.9$ electrons is obtained.[22] This result strongly suggests that the catalytic reduction is mainly from $[NO_2]^-$ to $NH_2OH$ (4 electrons) and/or $NH_2NH_2$ (5 electrons per nitrogen) and/or $NH_3$ (6 electrons) with little or no involvement of the 2-electron-reduction product $N_2O$ or 3-electron-reduction product $N_2$.

Further, the shift of reduction peak potential with solution pH demonstrates that protonation steps are involved. Ideally, these products should be identified positively by mass spectroscopy etc.; however the instability of the surface catalyst makes it impossible to generate sufficient product to be analyzed (however, see section 4).

**3. NO Reduction.** While nitric oxide is not reduced at the bare electrode (Figure 8A), it is electrocatalytically reduced by surface-bound $Fe^{III}(AC)$ (**2**) (Figure 8B). The similarity between the cyclic voltammogram (Figure 8B) recorded in NO solution and that obtained in $[NO_2]^-$ solution (Figure 5C) provides confirmation that reduction proceeds from $[NO_2]^-$ via formation of NO during the multielectron nitrite reduction. The formation of an iron nitrosyl derivative is a generally recognized step in the iron complex catalyzed reduction of $[NO_2]^-$:[4,7,9a,16,23]

$$[NO_2]^- + 2Fe^{II}L + 2H^+ \leftrightarrow ON\text{–}Fe^{II}L + Fe^{III}L + H_2O \quad (6)$$

On the electrode surface in the potential range for iron(II), the reaction should be

$$(Fe^{II}L)_{ad} + [NO_2]^- \leftrightarrow ([NO_2Fe^{II}L]^-)_{ad} \quad (7)$$

$$([NO_2Fe^{II}L]^-)_{ad} + e^- + 2H^+ \leftrightarrow (ON\text{–}Fe^{II}L)_{ad} + H_2O \quad (8)$$

where L refers to ligand.

**4. Detection of $NH_2OH$ and $NH_2NH_2$ Produced during the Reduction of $[NO_2]^-$ Using a Ring–Disk Electrode.** The possible products of $[NO_2]^-$ or NO reduction catalyzed by metal complexes have been determined to be mainly $N_2$, $N_2O$, $NH_2NH_2$, $NH_2OH$, and/or $NH_3$.[3-17]

In a ring–disk experiment, if any of these species are generated at the disk (coated with **2**), then they will, in principle, be detectable at the ring. This is a facile method of detecting and quantifying both $NH_2NH_2$ and $NH_2OH$, which can be oxidized at the ring. Figure 9 shows the oxidation of $NH_2NH_2$ (A), $NH_2OH$ (B), and $[NO_2]^-$ (C) on a rotating platinum ring electrode (during the measurements, the graphite disk electrode was kept open circuit—see Experimental Section). The fact that the oxidation currents for $NH_2NH_2$, $NH_2OH$, and $[NO_2]^-$ appear in different potential ranges (Figure 9) allows the quantities of $NH_2NH_2$ and $NH_2OH$ to be selectively determined.

A set of ring–disk-electrode experimental results are shown in Figure 10. Figure 10A is the response from the $[NO_2]^-$ reduction catalyzed by adsorbed **2** on the rotating graphite disk electrode. The peaklike current feature in Figure 10A instead of a plateau current reflects in part the loss of iron and may also signify formation of a noncatalytically active surface species when scanned more negative than −0.8 V. However some catalytic activity is recovered on the second and subsequent cycles.

If the platinum ring potential is fixed at 0.0 V, where only $NH_2NH_2$ could be oxidized (Figure 9A), no ring current is observed (Figure 10B); thus no detectable quantity of $NH_2NH_2$ is produced during the catalytic reduction of $[NO_2]^-$. However, if the ring potential is fixed at 0.5 V, where $NH_2OH$ could be oxidized without interference from the oxidation of substrate, $[NO_2]^-$, an oxidation current is observed (Figure 10C), demonstrating the formation of $NH_2OH$ during the catalytic reduction of $[NO_2]^-$.

The oxidation of $NH_2OH$ on a platinum electrode (Figure 9B) is a 2-electron-transfer process.[24] Thus, if the collection efficiency of the ring–disk electrode (calibrated with $K_4Fe(CN)_6$; see Experimental Section) is known, the data in Figure 10 can be used roughly to estimate the quantity of $NH_2OH$ produced in the reduction of $[NO_2]^-$. The area under the curve in Figure 10C corresponds to $1 \times 10^{-9}$ mol of $NH_2OH$, while the quantity of $[NO_2]^-$ reduced is about $2.5 \times 10^{-9}$ mol obtained from the area under the curve in Figure 10A, with the assumption of a 5-electron-reduction process. We have previously argued that both $N_2O$ and $N_2$ can only be minor products at the very best; thus, since $NH_2NH_2$ was not detected, the products of this reaction are approximately 40% $NH_2OH$ and 60% $NH_3$. Due to the loss of iron, it was not practical to build up a sufficient quantity of ammonia to detect it directly nor to exclude, positively, production of minor quantities of $N_2$ or $N_2O$.

**5. Discussion of the Catalytic Reduction Mechanism of $[NO_2]^-$.** A surface complex formed between the adsorbed metal–ligand complex and the substrate is generally recognized as the initial step of substrate reduction.[16] The evidence for surface complexes formed between adsorbed $Fe^{II}(AC)$ and solution $[NO_2]^-$ or NO is shown in Figure 11. The cyclic voltammogram in Figure 11A was recorded in pure supporting electrolyte after the electrode had been exposed to a solution of $Fe^{III}(AC)^-$. The wave near −0.2 V is the response for adsorbed $Fe^{III}(AC)/Fe^{II}(AC)^-$. When $1 \times 10^{-3}$ M $[NO_2]^-$ was added to the solution, there was a small

(22) Equations 3–5 are relevant to a simple irreversible reaction; the presence of a precomplexation step and the subsequent loss of iron from the electrode may introduce an error into this simple analysis. Although the data are in accord with eqs 3 and 4 to the extent of providing linear plots, the equations were not designed for the complex situation obtaining here, and the value of $n = 4.9$ may not be accurate.

(23) Zhang, V.; Kotowski, M.; Eldik, R. V. *Inorg. Chem.* **1988**, *27*, 3279.

(24) Karabinas, P.; Wolter, O.; Heitbaum, J. *Ber. Bunsen-Ges. Phys. Chem.* **1984**, *88*, 1191.

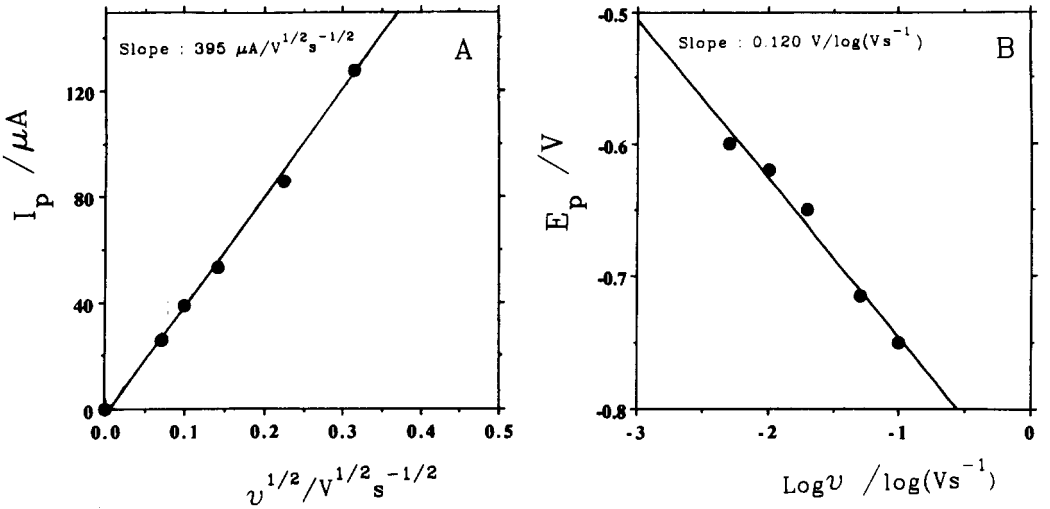


**Figure 7.** (A) Magnitude of the peak current, $i_p$ (ca –0.6 V), for $[NO_2]^-$ reduction in a $8 \times 10^{-4}$ M $NaNO_2$ solution from Figure 6 as a function of square root of scan rate and (B) peak potentials of $8 \times 10^{-4}$ M $NaNO_2$ reduction shown in Figure 6 as a function of logarithm of scan rates.

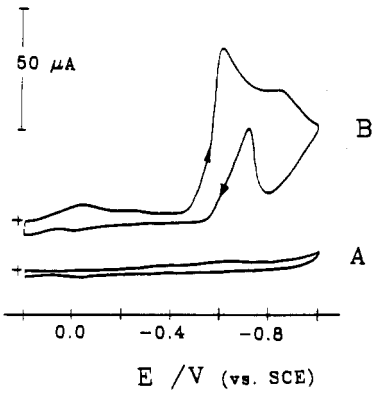


**Figure 8.** Cyclic voltammograms for the reduction of NO at a graphite electrode: (A) bare and (B) $Fe^{III}(AC)$ modified electrodes. The electrolyte solution was bubbled with NO gas for 1 min. $[Fe^{III}(AC)] = 3 \times 10^{-10}$ mol cm$^{-2}$. Supporting electrolyte was as in Figure 1 (pH 5.3) (first scan). Potential scan rate: 20 mV s$^{-1}$.

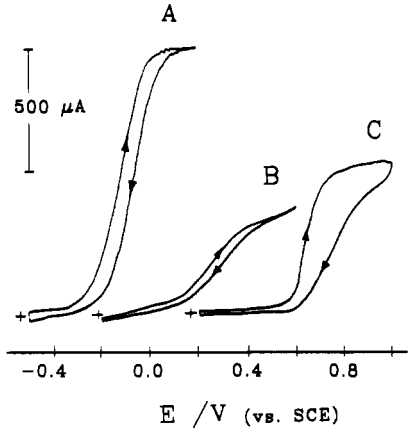


**Figure 9.** Current–potential curves for $1 \times 10^{-3}$ M (A) $NH_2NH_2$, (B) $NH_2OH$, and (C) $NaNO_2$ on a platinum ring electrode. Rotation rate: 400 rpm. Potential scan rate: 20 mV s$^{-1}$. Supporting electrolyte was as in Figure 1 (pH 5.3). Area of ring electrode: 0.11 cm$^2$.

shift of some 10–20 mV, possibly indicative of formation of an $NO_2^-$–Fe complex on the surface (Figure 11B).

In the presence of NO (about $1.5 \times 10^{-3}$ M), a new wave appears near –0.1 V attributable to formation of a surface nitrosyl complex. It is therefore evident that a nitrosyl complex is not *directly* formed when $[NO_2]^-$ contacts the surface species **2**. However, when the electrode was polarized to values where the $[NO_2]^-$ was reduced, the cyclic voltammogram, Figure 11D, was

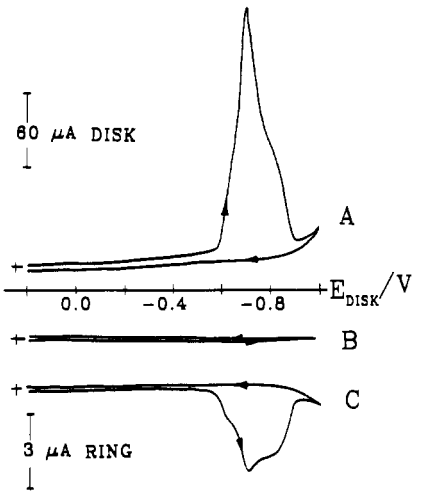


**Figure 10.** (A) Disk current–potential curve for the reduction of $5 \times 10^{-3}$ M $NaNO_2$ at a rotating platinum ring–graphite disk electrode, with the disk modified with $3 \times 10^{-10}$ mol cm$^{-2}$ $Fe^{III}(AC)$. (B) Ring current curve at ring potential of 0.0 V. (C) Ring current curve at ring potential of 0.5 V. Rotation rate: 400 rpm. Potential scan rate: 20 mV s$^{-1}$. Supporting electrolyte was as in Figure 1 (pH 5.3). Area of disk electrode: 0.46 cm$^2$. Ring collection efficiency: 0.15.

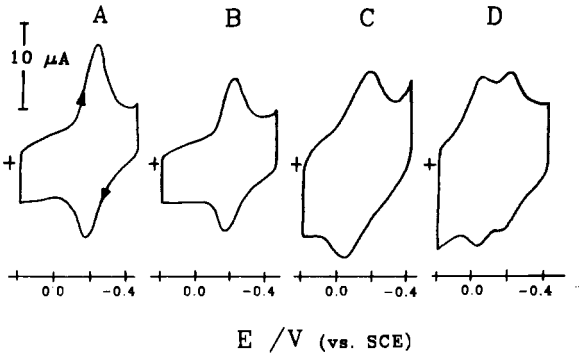


**Figure 11.** Cyclic voltammograms for $3.5 \times 10^{-10}$ mol cm$^{-2}$ $Fe^{III}(AC)$ modified graphite electrodes in (A) pure supporting electrolyte, (B) $1 \times 10^{-3}$ M $NaNO_2$, (C) about $1.5 \times 10^{-3}$ M NO, and (D) $1 \times 10^{-3}$ M $NaNO_2$ after the potential had been scanned to –1.0 V. Supporting electrolyte was as in Figure 1 (pH 5.3) (first scan). Potential scan rate: 100 mV s$^{-1}$.

obtained under the same scan conditions as those of Figure 11A,B. The obvious difference from Figure 11A,B is that a new wave appears near –0.05 V, which is considered to be the response from the product formed after $[NO_2]^-$ reduction when the surface

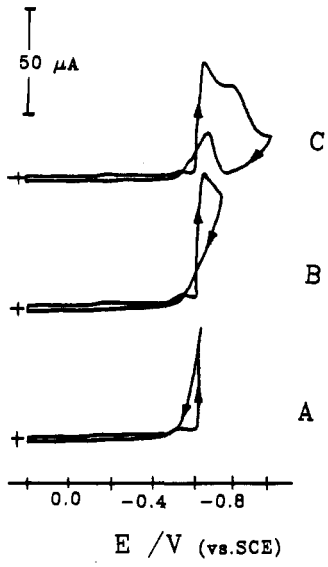


**Figure 12.** Cyclic voltammograms of $8 \times 10^{-4}$ M $NaNO_2$ reduction at a $Fe^{III}(AC)$ modified graphite electrode, where $[Fe^{III}(AC)] = 3 \times 10^{-10}$ mol $cm^{-2}$, with varying switching potential limits: (A) –0.65 V; (B) –0.75 V; (C) –0.98 V. Supporting electrolyte was as in Figure 1 (pH 5.3) (first scan). Potential scan rate: 20 mV $s^{-1}$.

is modified; it is presumably a nitrosyl derivative and probably the same species as that noted above, generated in the presence of NO.

In $1 \times 10^{-3}$ M $NH_2NH_2$, $1 \times 10^{-3}$ M $NH_2OH$, or $1 \times 10^{-3}$ M $NH_3$ solutions, the $Fe^{III}(AC)$ modified electrode did NOT show the electrochemical response at –0.05 V (as Figure 11D), indicating that these species are not responsible for the –0.05 V wave.

Further, no catalytic current waves were observed when a species **2** modified electrode was scanned in solutions of $NH_2$-$NH_2$ or $NH_2OH$, demonstrating that the reduction from $[NO_2]^-$ or NO to $NH_3$ does not proceed via $NH_2NH_2$ or $NH_2OH$.

Another unusual feature shown in Figure 5C and 8B is the additional reduction current near –0.7 V observed when the potential is scanned back to positive potentials. Thus, in the reduction of both $[NO_2]^-$ and NO there is at least one other product species which is reducible when the potential is scanned back.

Upon variation of the switching potential (Figure 12), it is evident that this reducible product exists throughout the whole potential range of $[NO_2]^-$ reduction. However, when the electrode was rotated, this back-reduction current disappeared, as shown in Figure 10A. Thus the product is a mobile species, not a surface species. It has not yet proven possible to identify this species.

**6. Structure of the Iron–AC Complex and Its Catalytic Activity.** The important structural feature of the AC ligand is the strong complexation of $Fe^{III}$ and $Fe^{II}$ by the (methylimino)diacetate group adjacent to one of the hydroxyl groups of catechol. It is this unit which is believed to be responsible for the electrocatalytic activity for $[NO_2]^-$ or NO reduction. The formation of $Fe^{II}$-(AC)–$[NO_2]^-$ and $Fe^{III}(AC)$–NO complexes can occur because there are two coordination sites available (occupied by water molecules)[20] for $[NO_2]^-$ or NO binding as in the case for $O_2$ or $H_2O_2$ reduction.[18]

In order to emphasize the importance of this structural feature, the $Fe^{III}$ complexes of four additional ligands with the same functional group, as noted in Figure 13, were investigated. These are also strongly adsorbed on graphite electrodes and act as electrocatalysts for the reduction of $[NO_2]^-$ (Figure 13). Thus the combination of a (methylimino)diacetate group and an adjacent phenolic hydroxyl group is sufficient to obtain catalytically active complexes with $Fe^{III}$.

**7. Possible Application of Species 2 for $[NO_2]^-$ or NO Analysis.** The concentration dependence of the peak current in cyclic

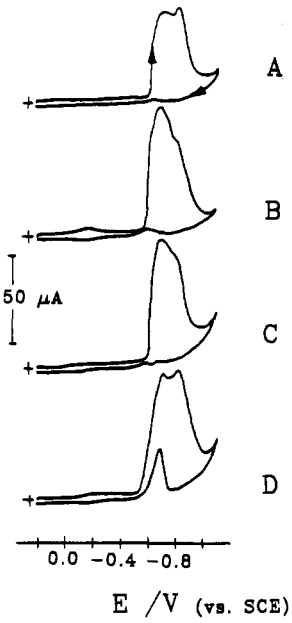


**Figure 13.** Cyclic voltammograms for the reduction of $1 \times 10^{-3}$ M $NaNO_2$ at graphite electrodes coated with the $Fe^{III}$ complexes of ligands (A) xylenol orange, (B) methylthymol blue, (C) fluorexon, and (D) thymolphthalein complexone. Supporting electrolyte was as in Figure 1 (pH 5.3) (first scan). Potential scan rate: 20 mV $s^{-1}$.

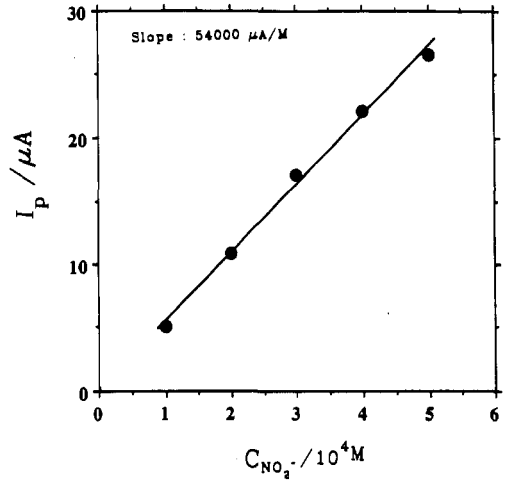


**Figure 14.** Concentration dependence of peak currents in cyclic voltammograms for the reduction of $NaNO_2$ at a $Fe^{III}(AC)$ modified graphite electrode, where $[Fe^{III}(AC)] = 3 \times 10^{-10}$ mol $cm^{-2}$. Supporting electrolyte was as in Figure 1 (pH 5.3). Potential scan rate: 20 mV $s^{-1}$. A fresh surface was used for each experiment to avoid problems due to loss of iron from the surface.

voltammograms for $[NO_2]^-$ reduction in solution was examined (Figure 14). The minimum concentration of $[NO_2]^-$ detectable by this electrocatalytic method by the adsorbed $Fe^{III}(AC)$ complex is about $1 \times 10^{-4}$ M (about 5 ppm). The low sensitivity may be attributed to the fact that there must be enough $[NO_2]^-$ existing in the solution to form an adduct with the adsorbed $Fe^{II}(AC)$ complex. The sensitivity may be improved by the use of different electrochemical measurement methods. The excellent linear relationship shown in Figure 14 is indicative of the possible application in $[NO_2]^-$ or NO analysis when a suitable protective coating is identified. However above 0.6 mM $[NO_2]^-$ there is deviation from linearity.

Various ions were tested as potential interferences in the nitrite reduction. The halides, $CO_3^{2-}$, $SO_4^{2-}$, $NO_3^{2-}$, $CO_2$, and CO have no effect upon nitrite reduction. Sulfite can be reduced on both bare and $Fe^{III}(AC)$ coated electrodes beginning at –0.6 V in a pH 5.3 solution containing sulfite anions with almost the same current magnitude in both situations; i.e., the Fe(AC) species is

not electrocatalytic. However sulfite will be an interference unless its concentration is known. Strongly binding ions such as $CN^-$, $SCN^-$, and $HS^-$ exert a very strong poisoning effect upon the electrocatalyst by binding to the available sites.

## Conclusion

The strong and irreversible adsorption of $Fe^{III}(AC)$ on graphite electrodes produces a surface with interesting electrocatalytic activity toward the reduction of nitrite and nitric oxide. However it is not active for the electroreduction of $NH_2OH$ or $NH_2NH_2$. The products of the electrocatalytic reduction of nitrite could be detected *in situ* by the rotating ring–disk electrode method. The main products were identified as $NH_2OH$ (40%) and $NH_3$ (60%).

The initial steps in the nitrite reduction mechanism are believed, from surface cyclic voltammetric behavior, to be the formation of adducts between substrate and adsorbed catalyst, possibly $O_2N^-$–$Fe^{II}(AC)$ and ON–$Fe^{II}(AC)$.

The combination of a (methylimino)diacetate group adjacent to a phenolic hydroxyl group present in the alizarin complexone was shown to be important to obtain an adsorbed complex which is catalytically active toward the reduction of nitrite and nitric oxide.

**Acknowledgment.** We are indebted to the Natural Sciences and Engineering Research Council for a Strategic Grant supporting this work and to Professor F. C. Anson for useful discussions.